Peroxidases Inhibit Nitric Oxide (NO) Dependent Bronchodilation: Development of a Model Describing NO−Peroxidase Interactions†

Husam M. Abu-Soud,*,‡ Mohamed Y. Khassawneh,§ Ju-Tae Sohn,|| Paul Murray,|| Musia A. Haxhiu,§ and Stanley L. Hazen*,‡,⊥

Departments of Cell Biology, Research Anesthesia, and Cardiology and Center for Cardiovascular Diagnostics and Prevention, Cleveland Clinic Foundation, Cleveland, Ohio 44195, Division of Pulmonary Medicine, Case Western Reserve University, Cleveland, Ohio 44195, and Chemistry Department, Cleveland State University, Cleveland, Ohio 44115

Received June 12, 2001; Revised Manuscript Received August 3, 2001

ABSTRACT: Recent studies demonstrate that nitric oxide (NO) serves as a physiological substrate for mammalian peroxidases [(2000) *J. Biol. Chem. 275*, 37524]. We now show that eosinophil peroxidase (EPO) and lactoperoxidase (LPO), peroxidases known to be enriched in airways of asthmatic subjects, function as a catalytic sink for NO, modulating its bioavailability and function. Using NO-selective electrodes and direct spectroscopic and rapid kinetic methods, we examined the interactions of NO with EPO and LPO compounds I and II and ferric forms and compared the results to those reported for myeloperoxidase. A unified kinetic model for NO interactions with intermediates of mammalian peroxidases during steady-state catalysis is presented that accommodates unique features observed with each member of the mammalian peroxidase superfamily. Potential functional consequences of peroxidase−NO interactions in asthma are investigated by utilizing organ chamber studies with tracheal rings. In the presence of pathophysiologically relevant levels of peroxidases and H_2O_2, NO-dependent bronchodilation of preconstricted tracheal rings was reversibly inhibited. Thus, NO interaction with mammalian peroxidases may serve as a potential mechanism for modulating their catalytic activities, influencing the regulation of local inflammatory and infectious events in vivo.

Nitric oxide (NO,[1] nitrogen monoxide) plays important physiological roles in airway function (*1*−*4*). This gaseous signaling molecule is generated by a family of enzymes named nitric oxide synthases (NOSs), which catalyze the conversion of L-arginine, molecular oxygen, and NADPH into NO and citrulline (*5*). During asthma, enhanced production of NO, a potent bronchodilator, is observed (*6*−*9*). And yet, reversible obstructive airway disease and bronchoconstriction are defining clinical features of the disorder (*10*). The apparent functional deficiency of NO and NO-releasing substances (e.g., GSNO) in asthma and other inflammatory conditions has been attributed to enhanced rates of NO consumption through oxidative processes within airway tissues (*1*−*4*, *11*−*14*); however, the pathways that promote accelerated consumption of NO during asthma are not established.

A major pathway for NO removal in vivo under physiological conditions is through interaction with oxyhemoglobin, yielding methemoglobin and nitrate (NO_3^-) (*15*). In addition, autoxidation of NO by slow interaction with molecular oxygen (O_2) in aqueous solutions leads to the formation of nitrite (NO_2^-) as a primary end product (*16*, *17*). However, neither of these pathways for NO removal is likely enhanced at sites of airway inflammation in asthma. One likely mechanism for accelerated NO catabolism is through the near diffusion-limited interaction of NO with $O_2^{\bullet-}$, yielding peroxynitrite ($ONOO^-$) (*18*, *19*). This potent oxidant is capable of promoting both protein nitration (*18*−*21*) and initiation of lipid peroxidation (*22*−*25*), processes known to occur during asthma (*11*, *12*, *14*, *26*−*28*). NO may also be consumed by radical−radical coupling reactions with lipid alkoxyl and peroxyl radicals, species formed during lipid peroxidation (*13*, *14*, *18*, *19*, *25*). Alternative oxidative pathways may also participate in depletion of NO in airway tissue during asthma. For example, recent in vitro studies suggest that NO can be consumed by lipoxygenases through interaction of NO with an intermediate radical species generated during lipoxygenase catalysis (*29*). Whether or not alternative mechanism(s) exist for the catabolism of NO at sites of inflammation is still unclear.

† This work was supported in part by National Institutes of Health Grants HL62526, HL61878 (S.L.H.), and HL66367 (H.M.A.-S.).

* Address correspondence to S.L.H. and H.M.A.-S. at the Department of Cell Biology, Lerner Research Institute, Cleveland Clinic Foundation, 9500 Euclid Ave., NC-10, Cleveland, OH 44195. Tel: (216) 445-9763. Fax: (216) 444-9404. E-mail: hazens@ccf.org; abusouh@ccf.org.

‡ Department of Cell Biology, Cleveland Clinic Foundation.

§ Division of Pulmonary Medicine, Case Western Reserve University.

|| Department of Research Anesthesia, Cleveland Clinic Foundation.

⊥ Department of Cardiology and Center for Cardiovascular Diagnostics and Prevention, Cleveland Clinic Foundation, and Chemistry Department, Cleveland State University.

[1] Abbreviations: EFS, electric field stimulation; EPO, eosinophil peroxidase; Fe(III), ferric; Fe(II), ferrous; HRP, horseradish peroxidase; H_2O_2, hydrogen peroxide; KH, Krebs−Henseleit; LPO, lactoperoxidase; MPO, myeloperoxidase; NOS, nitric oxide synthase; NO, nitric oxide (nitrogen monoxide).

10.1021/bi011206v CCC: $20.00
Published on Web 09/08/2001

We have recently suggested that mammalian peroxidases, some of the most abundant proteins present in inflammatory cells, may serve as an alternative pathway for catalytic removal of NO at sites of inflammation and cardiovascular disease (*30*, *31*). Myeloperoxidase (MPO), eosinophil peroxidase (EPO), and lactoperoxidase (LPO) are members of the mammalian peroxidase superfamily and play specific and complementary roles in host defense (*32*, *33*). Although the three enzymes are distinct gene products and differ from each other with respect to their sites of expression, their primary sequences, and their substrate specificities, they are similar regarding catalysis (*34*−*38*). The three hemoproteins contain distinct prosthetic groups that attached to the enzyme through imidazole nitrogen and use H_2O_2 as the electron acceptor in the catalysis of oxidative reactions. The initial redox intermediate formed following addition of H_2O_2 to MPO is termed compound I. MPO compound I, a ferryl π-cation radical [MPO−Fe(IV)═$O^{\bullet+\pi}$] with a formal heme charge of +5, is capable of oxidizing cosubstrates such as Cl^- through a single $2e^-$ transition generating MPO−Fe(III) and the hypohalous acid HOCl (*39*, *40*). Alternatively, MPO compound I can oxidize multiple organic and inorganic compounds by two successive $1e^-$ transfers, generating radical species and the MPO intermediates compound II [MPO−Fe(IV)═O] and MPO−Fe(III), respectively (*37*, *38*, *41*). Both EPO and LPO share with MPO the ability to use multiple distinct low molecular weight targets as substrates for $1e^-$ and $2e^-$ oxidation reactions (*14*, *41*−*44*). Substrates used by EPO, LPO, and MPO for $2e^-$ redox reactions include halides and pseudohalides, forming hypohalous acids, potent oxidants with antimicrobial properties. In contrast to the preference of MPO for Cl^- (*37*−*41*), at plasma levels of halides, EPO preferentially uses Br^- and the pseudohalide thiocyanate (SCN^-) as cosubstrate to form HOBr (*42*−*44*) and HOSCN (*45*), respectively, while LPO only utilizes SCN^- (*46*).

Recent studies demonstrate that MPO (secreted from activated neutrophils and monocytes) and EPO (secreted from activated eosinophils) both catalyze oxidative modification of proteins within asthmatic airways of humans following allergen challenge (*47*) and during exacerbation (*26*). EPO, MPO, and LPO were also recently shown to utilize NO as a substrate (*31*). MPO was then used as a model peroxidase and shown to accelerate NO consumption even in the presence of an $O_2^{\bullet-}$ generating system and alternative cosubstrates (*31*). These results suggested that peroxidases might serve as a catalytic sink for NO. Neither the biological significance nor the interactions of NO with EPO and LPO have been examined in detail.

In the present study we examine the potential physiological relevance of peroxidase−NO interactions as they may relate to asthma. First, we utilize rapid kinetic methods to characterize NO interactions with various forms of EPO and LPO, peroxidases enriched in asthmatic airways (*48*−*51*), during steady-state catalysis. A comprehensive kinetic model that describes the interactions between NO and mammalian heme peroxidases during steady-state catalysis is presented. Then, we utilize a NO-selective electrode to determine if EPO and LPO can augment NO decay rates in the presence of plasma levels of halides and an $O_2^{\bullet-}$-generating system. Finally, we examine the potential role of EPO and LPO in attenuating NO-dependent relaxation of tracheal rings, a process with important implications in asthma. On the basis of the present results and recent published findings we hypothesize that a complex bidirectional relationship exists between peroxidase activity and NO levels at sites of inflammation; NO serves to modulate peroxidase catalytic activity, while peroxidases serve as a catalytic sink for NO, influencing its bioavailability and function.

EXPERIMENTAL PROCEDURES

Materials. NO gas was purchased from Matheson Gas products, Inc., and used without further purification. For each experiment, a fresh saturated stock of NO was prepared under anaerobic conditions. The extent of nitrite/nitrate (NO_2^-/NO_3^-) buildup in NO preparations over the time course used for the present studies was <1−1.5% (per mole of NO), as determined by anion-exchange HPLC under anaerobic conditions (*31*). All other reagents and materials were of the highest purity grades available and were obtained from Sigma Chemical Co. (St. Louis, MO) or the indicated source.

General Procedures. Porcine EPO was isolated using a modification of the method of Jorg (*52*), as described (*53*) using guaiacol oxidation as the assay (*54*). EPO preparations were pure and were confirmed to be devoid of contaminating MPO by demonstrated by a RZ of >1.00 (A_{415}/A_{280}), SDS−PAGE analysis with Coomassie Blue staining, and in-gel tetramethylbenzidine peroxidase staining (*53*). Human MPO was purified as described (*55*). Trace levels of contaminating EPO were then removed by ion-exchange chromatography (*56*). MPO purity was established by demonstrating a RZ of >0.85 (A_{430}/A_{280}), SDS−PAGE analysis with Coomassie Blue staining, and in-gel tetramethylbenzidine peroxidase staining to confirm no contaminating EPO activity. Extinction coefficients of 89 000 and 112 000 M^{-1} cm^{-1}/heme of MPO (*57*) and EPO (*58*, *59*), respectively, were used. Bovine LPO was obtained from Worthington Biochemistry Corp. (Lakewood, NJ) and used without further purification. Purity was confirmed by demonstrating a RZ of >0.75 (A_{412}/A_{280}) and SDS−PAGE analysis.

Spectroscopy. Anaerobic spectra of EPO and LPO forms were recorded in septum-sealed quartz cuvettes equipped with a quick-fit joint for attachment to a vacuum system. Peroxidase samples were made anaerobic by repeated cycles of evacuation and equilibrated with catalyst-deoxygenated N_2. Cuvettes were maintained at 25 °C under N_2 or NO atmosphere during spectral measurements.

Stopped-Flow Measurements. The kinetics of EPO and LPO compound II formation and decay in the absence and presence of different NO concentrations were performed using a dual syringe stopped-flow instrument obtained from Hi-Tech Ltd. (model SF-51). Experiments were initially preformed under conditions identical to that recently reported for MPO (*30*, *31*) to facilitate comparisons. Measurements were carried out under anaerobic atmosphere at 25 °C following rapid mixing of equal volumes of an H_2O_2-containing buffer solution and a peroxidase solution that contained different NO concentrations. Reactions were monitored at 445 nm for EPO (an isosbestic point of compound I and EPO ground state) and 430 nm for LPO (an isosbestic point of compound I and LPO ground state). The time course of absorbance change was fit to either single- ($Y = 1 - e^{-kt}$) or double-exponential ($Y = Ae^{-k_1 t} + Be^{-k_2 t}$)

functions as indicated. Signal-to-noise ratios for all kinetic analyses were improved by averaging at least six to eight individual traces. In some experiments the stopped-flow instrument was attached to a rapid scanning diode device (Hi-Tech MG-6000) designed to collect 96 complete spectra in a specific time frame. The diode array detector was calibrated relative to four reference absorbance wavelengths (362, 420, 466, and 536 nm) of a holmium oxide filter. Rapid scanning experiments involve mixing solutions of peroxidase (3 μM) with buffer solutions containing 40 μM H_2O_2 at 10 °C.

NO-Selective Electrode Measurements. NO measurements were carried out using an NO-selective electrode (ISO-NO Mark II, World Precision Instruments, Sarasota, FL) connected to a chart recorder. Experiments were performed at 25 °C by immersing the electrode in 10 mL of 0.2 M sodium phosphate buffer, pH 7.0, under air. NO was added to a continuously stirred buffer solution from an anaerobic NO-saturated stock, and the rise and fall in NO concentration were continuously monitored. To determine the effect of H_2O_2 and peroxidases on NO levels during steady-state catalysis, 10 μL of H_2O_2 (100 μM final) and 50 μL of enzyme (150 nM final) were added to the reaction mixture. Where indicated, solutions were supplemented with plasma levels of halides (100 mM Cl^-, 100 μM Br^-) and/or a cell-free $O_2^{\bullet-}$ -generating system comprised of lumazine (0.4 mm) and bovine milk xanthine oxidase (XO, Boehringer Mannheim). Superoxide generation under the conditions utilized was ~40 μM/min, as measured by the superoxide dismutase-inhibitable reduction of ferricytochrome *c* (*60*).

Tracheal Ring Studies. Normal rats were sacrificed and their trachea removed. Under the dissecting microscope each trachea was freed of adventitia and fat tissue. A cylindrical airway segment of 3 mm length was isolated from the midtrachea of each animal and placed in a modified Krebs−Henseleit (KH) solution of the following composition (mM): NaCl, 118.2; $NaHCO_3$, HCl, 4.6; KH_2PO_4, 1.2; $MgSO_4$, 1.2; $CaCl_2$; and dextrose, 10%, with a pH adjusted to 7.4. The solution was continuously aerated with 5% CO_2 balanced with O_2. Tracheal cylinders were suspended between a sturdy glass rod and a force displacement transducer (FT 03, Grass Instruments, Quincy, MA) connected to an amplifier as previously described (*61*, *62*). Generated forces were continuously monitored and recorded on a rectilinear chart recorder. The cylinders were allowed to equilibrate in the organ bath (Radnoti Glass, CA) for 40−45 min before challenge. The optical length at which maximal isometric force developed was obtained for each cylinder by 0.1 g increments of load until electrical field stimulation (5 V dc applied through platinum electrodes, 250 mA/cm^2) applied for 10 s at 4 min intervals gave a reproducible maximal response.

A cumulative concentration−response curve to bethanecol (3×10^{-8} to 10^{-3} M) was obtained for each cylinder. The concentration of bethanecol that elicited 50−75% of maximal response (ED 50−75) was determined. The airway cylinders were then washed, equilibrated, and precontracted with bethanecol (ED 50−75: between 3×10^{-6} and 10^{-5} M). Electrical field stimulation (EFS) was then applied to each precontracted cylinder at a range of 0.5, 1, 2, 4, 8, 16, 32, and 64 Hz at a constant voltage (5 V) and dc current. The percent relaxation from the precontracted state was calculated for each cylinder. The percent relaxation in response to EFS was calculated from the reduction in tension (in grams) in relation to baseline tension in the precontracted state, each tracheal segment serving as its own control (before and after EFS exposure). All stock solutions were made freshly on the day of the experiments. Stock solution of oxidases (H_2O_2-generating system) and peroxidases were made in KH buffer. Where indicated, a continuous flux of H_2O_2 was generated with the glucose (0.6 mM final)/glucose oxidase (200 ng/mL) system. Under these conditions, a continuous flux of H_2O_2 is formed (~1.8 μM/min). Bethanechol was dissolved in distilled water. PGE2 was dissolved in 0.1 M phosphate buffer (pH 7.0) solution.

RESULTS

Spectroscopic and Rapid Kinetics Characterization of the Interaction between NO and Compounds I and II of EPO and LPO. EPO and LPO are enriched in inflamed airways of asthmatic subjects, and yet the interactions of NO with these enzymes have not been examined in detail. Rapid mixing of a solution of EPO−Fe(III) with an equal volume of a 20-fold molar excess of H_2O_2 in the absence of cosubstrates resulted in the rapid formation of a transient complex that displayed a Soret absorbance at 413 nm and broad visible bands centered at 598 and 668 nm (data not shown), typical of a six-coordinate complex. This spectrum differs from that of either ferric or ferrous EPO, whose Soret maxima are centered at 413 and 450 nm, respectively. The spectrum of the intermediate initially formed following addition of H_2O_2 to EPO−Fe(III) is consistent with formation of EPO compound I (*63*) and similar to that of LPO and MPO compound I (*64*−*67*). This EPO intermediate formed within 50 ms after mixing at 25 °C but was unstable and rapidly converted into a more stable intermediate within 3 s, as judged by a time-dependent shift in Soret absorbance from 413 to 432 nm. This species displayed a Soret band at 432 nm and two visible bands at 532 and 564 nm, consistent with formation of EPO compound II, as shown in Figure 1. EPO compound II is also unstable and converted gradually to the ground state, EPO−Fe(III), within minutes of initiating the reaction (Figure 1). Spectral transitions between each intermediate formed revealed distinct and well-defined isosbestic points (Figure 1). Thus sequential formation and decay of EPO intermediates within the peroxidase cycle occur at sufficiently different rates to enable each process to be studied by conventional (i.e., single mixing) stopped-flow methods. Addition of H_2O_2 to LPO−Fe(III) in the absence of cosubstrates similarly leads to the accumulation of compound II in the millisecond time frame via transient initial formation of compound I and subsequent spontaneous $1e^-$ heme reduction, similar to that observed with EPO and MPO (*63*−*67*).

We next utilized stopped-flow spectroscopy to investigate how NO interacts with intermediate forms of EPO and LPO during steady-state catalysis. The influence of NO on the kinetics of EPO and LPO compound II buildup, duration, and decay was examined under anaerobic conditions following rapid mixing of enzyme and various concentrations of NO in the presence of physiological concentrations of H_2O_2 (10 μM final). The time courses for the formation and decay of compound II of both EPO and LPO in the absence of NO were detected by monitoring the absorbance change

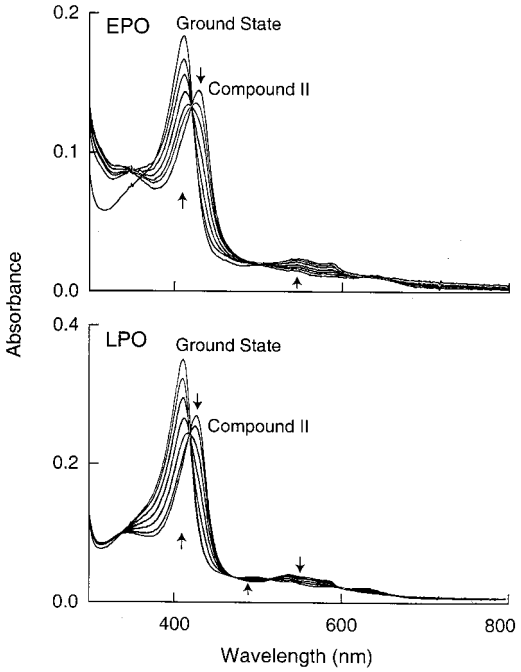

FIGURE 1: Formation of EPO and LPO compound II and subsequent conversion to ground state in the absence of NO. Cuvettes contained 1.5−2 μM EPO (upper panel) or LPO (lower panel) in phosphate buffer (200 mM, pH 7.0) under aerobic atmosphere at 25 °C. Reactions were initiated by adding 50 μM H_2O_2. Spectral traces were recorded immediately after initiating the reaction (spectra of compound II) and then after every 2 min for EPO and after every 3 min for LPO up to 60 min. Some of the spectra recorded between the 0 and 60 min scans were omitted from each panel for clarity. Arrows indicate the direction of spectral change over time as compound II of each peroxidase decays to its ferric form.

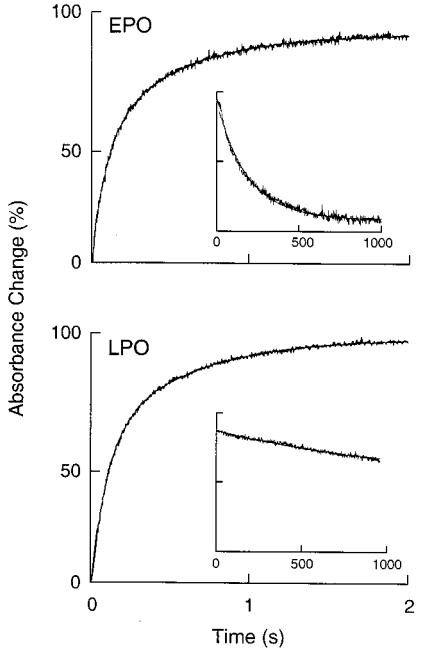

FIGURE 2: Stopped-flow measurements of EPO and LPO compound II formation and decay following addition of H_2O_2. An anaerobic solution containing sodium phosphate buffer (200 mM, pH 7.0) supplemented with H_2O_2 (20 μM) was rapidly mixed with an equal volume of buffer supplemented with either 0.86 μM EPO−Fe(III) (upper panel) or 0.86 μM LPO−Fe(III) (lower panel) at 25 °C. Spectral changes were monitored as a function of time at 445 nm for EPO and 430 nm for LPO, characteristic wavelengths for compound II of each peroxidase. Insets are expanded time courses of compound II formation and subsequent decay upon addition of H_2O_2 to either EPO or LPO. The formation and the decay of EPO and LPO compound II were best fit to single-exponential functions (solid lines).

at 445 nm for EPO and at 430 nm for LPO (Figure 2). For both enzymes, the changes in absorbance that take place in the first 2 s of the reactions are shown and are attributed to the buildup of compound II. The buildup of compound II of both EPO and LPO was best fit to a single-exponential function, giving apparent pseudo-first-order rate constants of 4.3 s^{-1} and 4.6 s^{-1}, respectively. The subsequent decreases in absorbance at 455 and 430 nm observed for both enzymes were also fit to a single-exponential function with a rate constant of 0.005 s^{-1} for EPO and 0.0005 s^{-1} for LPO (Figure 2, insets). These spectral changes were attributed to the decay of compound II of EPO and LPO. Together, these results indicate that the buildup rates of compound II formation for each enzyme in the absence of NO is rapid, monophasic, and occurs with a much faster rate than its decay.

The addition of NO to reaction mixtures of EPO or LPO results in dramatic effects on the rates of compound II buildup, duration, and decay, as assessed by stopped-flow spectroscopy (Figure 3). For both enzymes, NO was readily used as a $1e^-$ substrate by compound I, as indicated by the enhanced rate of compound II formation (Figures 3 and 4). For EPO, the rate of compound II accumulation was enhanced nearly 25-fold in the presence of NO and increased in a concentration-dependent and saturable manner (Figure 4). In contrast, the rate of LPO compound II accumulation increased in a linear manner as a function of NO concentration (Figure 4), yielding a second-order rate constant of 2×10^6 M^{-1} s^{-1}. In addition, NO influenced the steady-state level of EPO and LPO compound II formed following H_2O_2

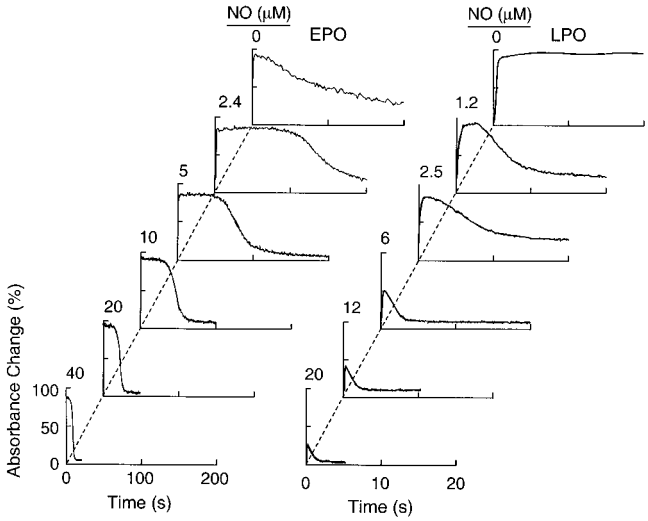

FIGURE 3: Effect of NO concentration on EPO and LPO compound II formation, duration, and decay during steady-state catalysis. Formation and decay of compound II of EPO (left panel) and LPO (right panel) were monitored as a function of time by observing spectral change at 445 and 430 nm, respectively. An anaerobic solution containing sodium phosphate buffer (200 mM, pH 7.0) supplemented with H_2O_2 (20 μM) was rapidly mixed with an equal volume of buffer containing either 0.86 μM EPO−Fe(III) or 0.86 μM LPO−Fe(III) and differing concentrations of NO at 25 °C. The final concentration of NO in mixtures is indicated.

addition. As the concentration of NO present in reaction mixtures was increased, the steady-state levels of LPO compound II generated progressively decreased, as judged

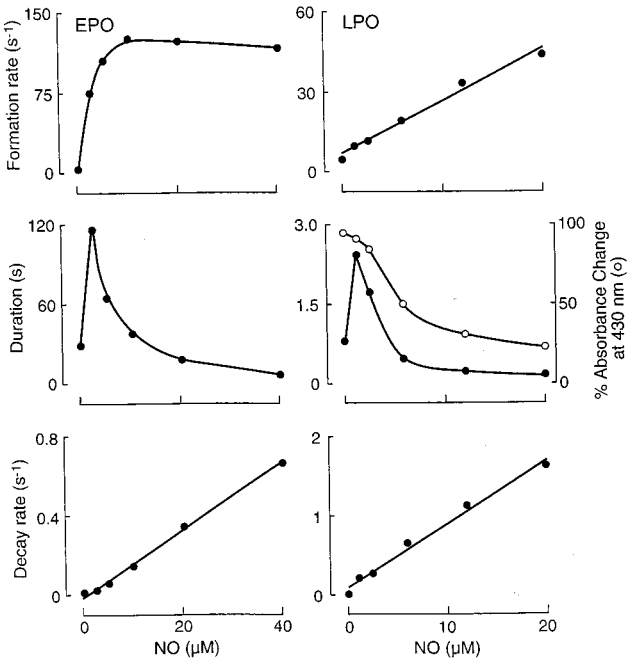

FIGURE 4: Rate of EPO and LPO compound II formation, duration, and decay as a function of NO concentration. The observed rates of EPO (left panel) and LPO (right panel) compound II formation, duration, and decay (monitored at 445 nm for EPO and 430 nm for LPO) observed in Figure 3 were plotted as a function of NO concentration. Data represent the mean of triplicate determinations from an experiment performed three times. The percent absorbance change at 430 nm is also shown for LPO compound II as a function of NO concentration (right panel, center).

by the decrease in overall absorbance at 430 nm developed during steady-state catalysis (Figures 3 and 4). The presence of NO had a variable effect on the duration of maintaining steady-state concentrations of compound II for each peroxidase following H_2O_2 addition (Figure 4). Finally, NO significantly accelerated the rate of compound II decay for both EPO and LPO in a concentration-dependent fashion. Plots of NO concentration vs observed rates of compound II decay for each peroxidase demonstrated linear kinetics and yielded second-order rate constants of 1.7×10^4 M^{-1} s^{-1} and 8.7×10^4 M^{-1} s^{-1} for EPO and LPO, respectively (Figure 4). The accelerated rate of compound II decay in the presence of NO indicates that NO also serves as a $1e^-$ substrate for both EPO compound II and LPO compound II.

NO Is Catalytically Consumed by Peroxidases Enriched in Asthmatic Airways under Physiological Conditions. We recently demonstrated that MPO accelerates NO removal from buffer in the presence of $O_2^{\bullet-}$ and plasma levels of halides (Cl^-, 100 mM; Br^-, 100 μM) (*31*). Using an NO-selective electrode, we performed similar studies and confirmed that catalytic amounts of EPO or LPO could accelerate NO consumption in the presence of $O_2^{\bullet-}$ and plasma levels of halides (data not shown). In both cases, the NO levels used were much less than the K_{diss} (k_{-1}/k_1) for LPO or EPO Fe(III)−NO (Table 1; *68*), which limits the interaction between NO and the enzymes. In control reactions lacking a $O_2^{\bullet-}$-generating system, neither peroxidases nor H_2O_2 alone significantly influenced the removal of NO. The present studies thus suggest a functional role for peroxidases as catalytic sinks for NO in inflamed airways.

Peroxidase/H_2O_2 Systems Reversibly Attenuate NO-Dependent Bronchodilation of Tracheal Rings. The rapid consumption of NO by mammalian peroxidases suggested that they might serve as a mechanism for modulating NO bioavailability and function in vivo. To examine the potential physiological relevance of peroxidase−NO interactions, we evaluated the capacity of EPO, LPO, and MPO to attenuate NO-dependent relaxation of tracheal rings. Experiments utilized precontracted tracheal rings to determine whether catalytic levels of peroxidases (e.g., data for EPO/H_2O_2 and LPO/H_2O_2 systems shown) inhibit NO-dependent bronchodilation. Briefly, different tracheal rings (Figure 5, data for four rings, R1−R4, shown) were isolated and precontracted with bethanecol (a long-acting cholinergic agent) that evoked a force of contraction of approximately 1 g. All rings were incubated in organ bath media in the presence of a slow flux of H_2O_2 (~1.8 μM/min) generated by the glucose/glucose oxidase system as described under Experimental Procedures. Control experiments demonstrated no significant effect of the H_2O_2-generating system on NO-dependent bronchodilation of the preconstricted rings (data not shown). Before NO exposure, R2 and R4 were treated with catalytic amounts of

Table 1: Kinetic Parameters for NO Binding to Ferric Forms of EPO, LPO, and MPO[a]

complexes	k_{on} (μM^{-1} s^{-1})	k_{off} (s^{-1})	ref
EPO−Fe(III) + NO	1.35	65	*68*
LPO−Fe(III) + NO	>3[a]	~1[b]	*68*
MPO−Fe(III) + NO	1.07	10.8	*30*

[a] The interaction of NO with Fe(III) forms of EPO, LPO, and MPO was studied at 10 °C in phosphate buffer, pH 7.0. The k_{on} and k_{off} were derived from the slope and intercept, respectively, following linear regression analysis of k_{obs} versus NO concentration. [a] NO binds to LPO−Fe(III) faster than the stopped-flow limits (2 ms dead time for acquisition) under the conditions employed. The reaction is reversible as judged by UV/vis studies. The rate constants presented are based on computer simulation of the kinetic data.

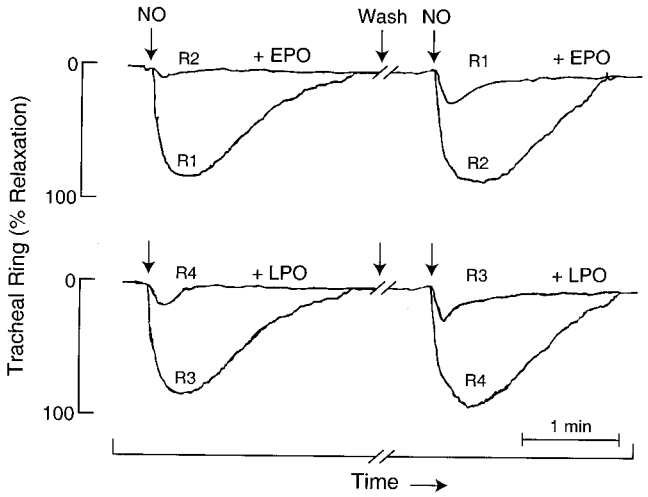

FIGURE 5: Peroxidase−H_2O_2 systems inhibit NO-dependent bronchodilation. The tracings from four typical tracheal rings (R1−R4) harvested from rats, transduced under tension, and contracted with bethanecol to 50−75% of tension are shown. Before first NO exposure, R2 and R4 were treated from the start with EPO−H_2O_2 and LPO−H_2O_2 systems, respectively, as described under Experimental Procedure, while R1 and R3 remained untreated (controls). NO (15 μM, final) was added to all ring baths 1 min following initiation of reactions, as indicated by the arrows. Where indicated, the organs were washed by KH and precontracted again with bethanecol. For the second NO exposure, R1 and R3 were treated from the start with EPO−H_2O_2 and LPO−H_2O_2 systems, respectively, while R1 and R2 were incubated in buffer only.

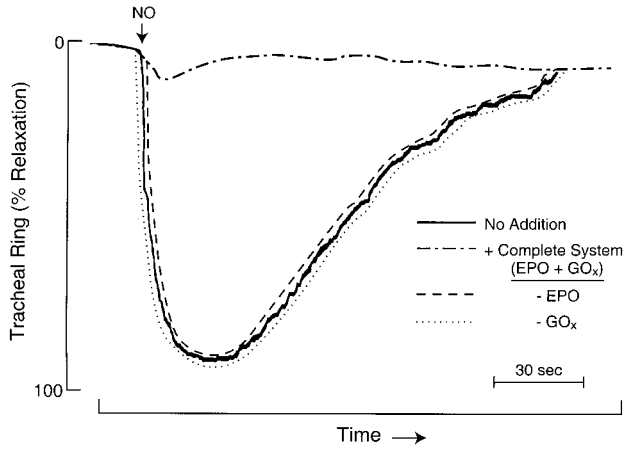

FIGURE 6: Attenuation of NO-mediated tracheal relaxation requires the combined presence of each component of the peroxidase−H_2O_2 system. Time-dependent NO-mediated (15 μM NO addition) relaxation of preconstricted tracheal rings was tested under four different conditions: (1) in the presence of no additives, (2) in the presence of a H_2O_2-generating system comprised of glucose/glucose oxidase (GOx: ~1.8 μM/min), (3) in the presence of EPO (150 nM), and (4) in the presence of both GOx and EPO (complete system).

either EPO or LPO while the control rings, R1 and R3, remain untreated. As expected, addition of NO to preconstricted tracheal rings in the absence of peroxidases (R1 and R3) resulted in the anticipated time-dependent bronchodilatory responses. In contrast, pretreatment of rings with catalytic levels of peroxidases (EPO and LPO, shown in R2 and R4 of Figure 5, respectively) dramatically attenuated the normally observed bronchodilation that follows addition of NO. Following a wash out period, rings previously treated with peroxidases (R2 and R4) again demonstrated NO-dependent bronchodilatory responses, confirming that the NO-dependent signaling pathways in the previously treated rings were still intact. Taken together, these experiments demonstrate that mammalian peroxidases and H_2O_2, components known to be enriched in asthmatic airways, can prevent NO-dependent bronchodilatory responses.

To further characterize the capacity of peroxidase−H_2O_2 systems to inhibit NO-mediated relaxation of tracheal rings, we examined the reaction requirements necessary for peroxidase-dependent inhibition of NO-mediated bronchodilatory responses. As shown in Figure 6, NO-mediated relaxation of tracheal rings occurred in the presence of either peroxidase or a H_2O_2-generating system but not the combined presence of both peroxidase and H_2O_2 (complete system).

We next quantified the effect of peroxidases on the concentration dependence of NO-mediated relaxation of preconstricted tracheal rings. Experiments were performed by equilibrating preconstricted tracheal rings in Krebs buffer supplemented with glucose/glucose oxidase (a H_2O_2-generating system; ~1.8 μM/min) and then assessing ring relaxation in response to varying amounts of NO in the absence and presence of specific peroxidases (EPO, LPO, or MPO). Typical NO-dependent relaxation curves of tracheal rings in the presence and absence of EPO and LPO are illustrated in Figure 7. In the absence of peroxidases, relaxation of the organ rings increases as a function of NO concentration and reaches a maximum at ~4 μM NO. In contrast, incubation of the tracheal rings with the bath media containing catalytic

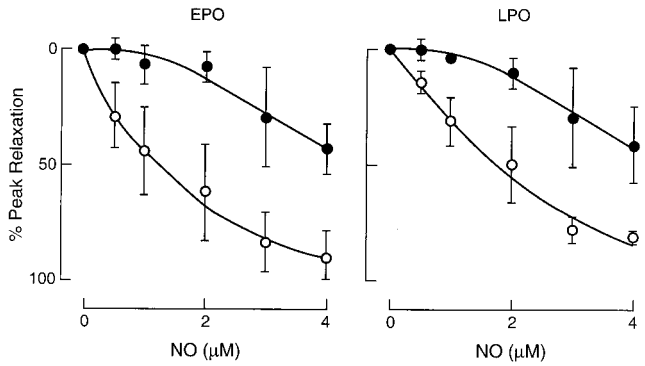

FIGURE 7: NO concentration−response curves for intact tracheal rings showing that peroxidase−H_2O_2 systems prevent NO-mediated relaxation. Precontracted tracheal rings were incubated in KH buffer in the presence of a H_2O_2-generating system (glucose/glucose oxidase; ~1.8 μM/min) in the absence (○) or presence (●) of EPO (left panel) or LPO (right panel). The effect of increasing NO concentrations on tracheal ring relaxation is shown. Data represent the mean ± SD of four independent experiments.

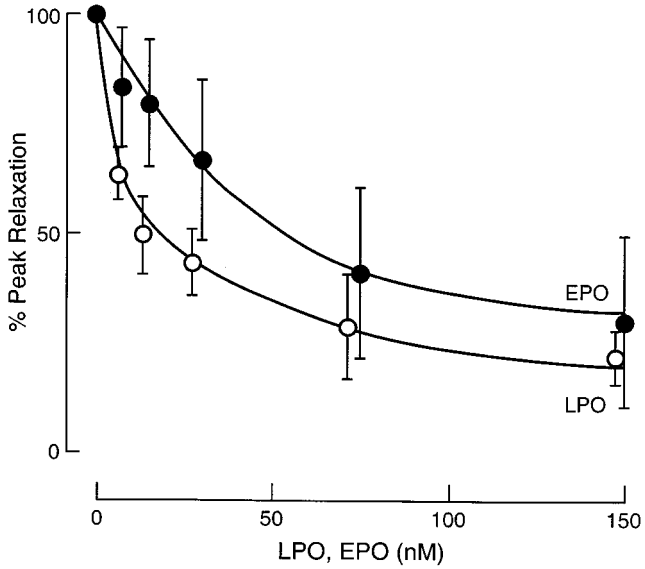

FIGURE 8: EPO and LPO concentrations modulate NO-induced relaxation of intact tracheal rings. The concentration dependence of EPO (●) or LPO (○) dependent inhibition of NO-meditated bronchodilation is shown. Experiments were performed under conditions similar to those used in Figure 7 except that a fixed (15 μM final concentration) level of NO was used in the presence of the indicated levels of peroxidase. Data are the mean ± SD of four experiments.

levels of peroxidase (data for EPO and LPO shown) attenuated NO-dependent relaxation, as reflected in the rightward shift of the dose−response curve. Finally, the concentration dependence of peroxidase-mediated inhibition of NO-triggered bronchodilation was assessed using preconstricted rat tracheal rings incubated with increasing concentrations of peroxidase in the presence of a fixed low flux (~1.8 μM) of H_2O_2 (Figure 8). Tracheal ring relaxation was achieved by exposing rings to fixed amounts of NO (15 μM). Increasing concentrations of peroxidase (data for EPO and LPO shown) significantly attenuated NO-mediated bronchodilation and reduced the maximal response to NO (Figure 8). Collectively, these results are consistent with peroxidases serving as a catalytic sink for NO, preventing tracheal relaxation.

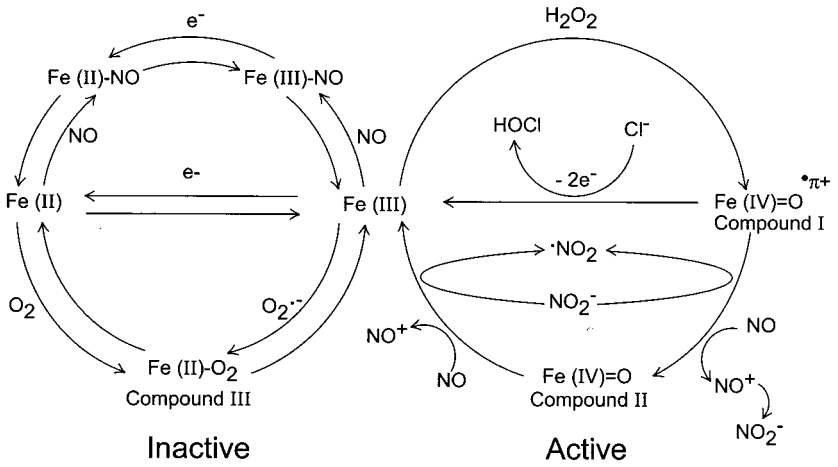

FIGURE 9: Comprehensive kinetic model for NO interactions with mammalian peroxidases.

DISCUSSION

Increased levels of NO, a potent bronchodilator, are typically observed in the exhaled breath of individuals with asthma (*4*, *6*−*9*, *69*). And yet, a functional deficiency of NO in airway tissues, as evidenced by bronchoconstriction, is a defining feature of the disease. This apparent paradox has led to the general belief that additional consumptive pathways for NO are operative in airway tissues during asthma, similar to that in other chronic inflammatory diseases (*3*, *4*, *11*−*14*). Thus, NO formed in airway epithelial cells may diffuse either into the airway lumen, where it escapes in exhaled breath, or into airway tissues, where it may be consumed prior to exerting it bronchodilator effect.

Most investigators have focused upon the potential role of $O_2^{\bullet-}$ interaction with NO-forming peroxynitrite ($ONOO^-$), a potent reactive nitrogen species, as a mechanism for NO removal and nitration of proteins (*11*−*14*, *18*−*22*). For example, immunohistochemical studies identified nitrotyrosine, a product formed by $ONOO^-$ interaction with tyrosine, as being enriched in asthmatic tissues (*11*, *12*, *26*) and airway proteins (*26*). However, we have recently examined the chemical pathways involved in oxidative modification of targets in asthmatic airways by NO-derived oxidants and proposed that EPO, an abundant peroxidase enriched and active in asthmatic airway tissues (*47*), serves as a major pathway for generating nitrotyrosine in airways of asthmatic subjects (*26*).

The results of the present study suggest that peroxidase−H_2O_2 systems may also serve as a catalytic sink for NO, limiting its bioavailability and function, such as in asthmatic airway tissues. Catalytic levels of peroxidases dramatically attenuated the capacity of NO to promote bronchodilatory responses (Figures 5−8). Moreover, peroxidase-dependent reversal of NO-mediated bronchodilation required active peroxidase and a physiological flux of the cosubstrate H_2O_2, consistent with the peroxidase−H_2O_2 system consuming NO before it diffused into the tissue. Increased levels of H_2O_2 are observed in breath condensates of individuals with asthma (*70*−*72*). Finally, the potential physiological relevance of this process was underscored using continuous monitoring of NO levels with an NO-selective electrode. EPO and LPO efficiently consumed NO in the presence of a cell-free $O_2^{\bullet-}$-generating system, even in the presence of plasma levels of halides. EPO, LPO, and MPO are all enriched in the airways of asthmatic subjects. We have recently demonstrated that the leukocyte peroxidases EPO and MPO contribute to inflammatory tissue injury via oxidative modification of targets in asthmatic airways following allergen challenge (*47*). The results of the present studies extend these observations and suggest that peroxidases may also participate in the disease process by serving as a catalytic sink for NO in airway tissues, limiting its bronchodilator actions.

In addition to the significant effects of peroxidases in modulating NO levels, NO serves to modulate peroxidase catalysis at multiple distinct levels. Identifying similarities and differences in the interactions between NO and various members of the mammalian peroxidase superfamily (e.g., EPO, LPO, and MPO) yields valuable mechanistic insights into the potential biochemical and functional significance of NO−peroxidase interactions in vivo. On the basis of the present results, recent published studies (*30*, *31*), and the affinities of Fe(III) (Table 1; *68*) forms of peroxidases for NO, we have generated a comprehensive kinetic model describing NO interactions with the catalytic intermediates of mammalian peroxidases that accommodates unique features observed with each member of the mammalian peroxidase superfamily (Figure 9). NO may partition between two cycles during steady-state catalysis of peroxidases: an active cycle that includes the ability of NO to influence compound II rates of formation and decay through its actions as a peroxidase substrate, and an inactive cycle that involves the formation of a ferric−nitrosyl [Fe(III)−NO] complex where NO serves as a ligand (Figure 9). The inactive cycle also includes heme reduction and the ability of Fe(II) and Fe(III) forms of heme peroxidase to bind to O_2 and $O_2^{\bullet-}$, respectively. This generates another intermediate, compound III, a ferrous−dioxy complex [Fe(II)−O_2], similar to oxyhemoglobin (Figure 9).

The relative affinity of the ground state (ferric) forms of peroxidases for either NO or H_2O_2, and the relative concentrations of NO vs H_2O_2, are what govern the overall partitioning of NO between these two cycles. In the presence of H_2O_2 and low NO concentrations [i.e., when NO levels are lower than the K_{diss} for Fe(III)−NO], NO predominantly serves as a $1e^-$ reductant for compounds I and II of peroxidases. The presumed intermediate formed, nitrosonium cation (NO^+), is extremely labile (half-life < 0.3 ns) and is rapidly hydrolyzed in aqueous solutions forming nitrite

(NO_2^-) (*73*). In support of this hypothesis, incubation of NO with H_2O_2 and either EPO, LPO (Abu-Soud and Hazen, unpublished results), or MPO (*31*) results in catalytic formation of NO_2^-. NO^+ was similarly recently suggested as the product generated following interaction of NO with a plant peroxidase, horseradish peroxidase (*74*). Formation of NO_2^-, a substrate for EPO (*26*, *53*), LPO (*74*), and MPO (*24*, *75*−*78*) at or near the heme moiety might thus also contribute to the increased overall transit time through the peroxidase cycle observed in the presence of NO. It also would serve to convert a relatively innocuous free radical species, NO, into a more noxious one, nitrogen dioxide ($^\bullet NO_2$) (Figure 9). $^\bullet NO_2$ generated by the MPO−H_2O_2−NO_2^- system of leukocytes promotes lipid peroxidation (*24*, *77*, *78*) and protein oxidation and nitration (*24*, *75*−*78*). Similar actions are likely with EPO and LPO (*14*, *26*, *53*, *75*).

The role of NO as a ligand for ferric and ferrous forms of hemoproteins such as hemoglobin, myoglobin, NOSs, and soluble guanylate cyclase is well documented (*79*−*84*). In a similar fashion, at higher levels of NO [i.e., when NO levels are higher than the K_{diss} for Fe(III)−NO], NO predominantly serves as ligand for Fe(III) forms (ground state) of peroxidases, generating their inactive Fe(III)−NO complexes (Figure 9). The relatively low affinity of EPO and MPO Fe(III) forms for NO at neutral pH (Table 1) suggests that the predominant effect of NO on catalysis by these leukocyte hemoproteins will be modulation of their activity (Figure 9). In contrast, LPO displays a high affinity for NO, and the predominant effect of NO in LPO-mediated catalysis is ligation of the heme into an inactive nitrosyl complex (Figure 9). The high dissociation rates of NO from EPO−Fe(III)−NO and MPO−Fe(III)−NO, relative to LPO−Fe(III)−NO (Table 1), also account for the differences in the observed plots of NO concentration vs rate of compound II formation (Figure 4) for the enzymes. For EPO (this study) and MPO (*30*, *31*), the rate-limiting step during steady-state catalysis shifts from reduction of compound II to dissociation of the Fe(III)−NO complex during steady-state catalysis and high levels of NO (Figure 9). Thus, the plot plateaus at a rate comparable to the temperature-adjusted dissociation rate constant for the respective Fe(III)−NO complexes. In contrast, the low dissociation rate of the LPO−Fe(III)−NO complex limits the amount of active peroxidase available during steady-state catalysis, and the plot of NO concentration versus rate of LPO compound II formation remains linear.

Finally, the present results suggest that a significant effect of NO−peroxidase interactions will be the modulation of the relative proportions of peroxidase intermediates available during steady-state catalysis. Compound II of peroxidases can only execute $1e^-$ oxidation reactions (*14*, *37*, *41*, *85*). Thus, formation of hypohalous acids is not possible with these intermediates. The results of the present study, in combination with recent studies with MPO (*30*, *31*), reveal that physiologically relevant levels of NO (low μM to nM, Figure 4) have significant effects on the rate of compound II formation, duration, and decay—and hence the steady-state levels of compound II. Thus, NO will effectively promote "substrate switching" for the peroxidases by influencing the ability of $1e^-$vs $2e^-$ reducing substrates to undergo catalysis.

To summarize, the present studies demonstrate a heretofore unrecognized bidirectional relationship between members of the mammalian peroxidase superfamily and NO (Figure 10). Using a combination of biochemical, physiological, and kinetic approaches, we show that peroxidases may serve as a catalytic sink for NO, limiting its bioavailability and function. NO consumption may be mediated by direct interaction of NO as a peroxidase substrate. It also may be mediated by indirect mechanisms through radical−radical coupling reactions with peroxidase-generated free radical species. In addition, NO will serve to modulate peroxidase catalytic activity by acting as both a ligand and a substrate. As a substrate, NO may accelerate the rate-limiting step in the peroxidase cycle, reduction of compound II, and enhance overall rates of catalysis (*30*). It also may modulate the distribution of peroxidase intermediates, compounds I and II, available during steady-state catalysis, hence affecting the substrate selectivity of the enzymes. Finally, NO can serve as a ligand for peroxidases, rendering them catalytically inactive. For the present studies we primarily focus on the interactions between NO, EPO, LPO, and tracheal rings using asthma as a model inflammatory disease for discussion. However, it should be noted that every member of the mammalian peroxidase superfamily examined thus far efficiently utilizes NO as a cosubstrate (*31*). Thus, mammalian peroxidases may participate in similar reactions at other sites of inflammation where leukocytes, peroxidases, and enhanced NO consumption are observed.

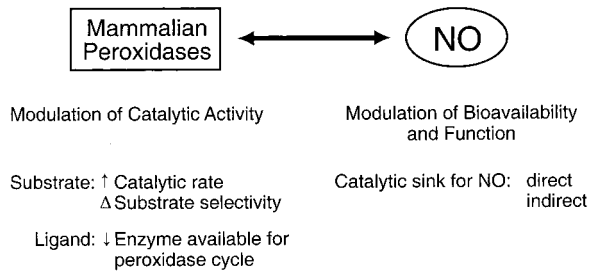

FIGURE 10: Scheme describing the bidirectional relationship between NO and peroxidases. Peroxidases may serve to modulate NO bioavailability and function by serving as a catalytic sink for NO. Peroxidases directly promote NO consumption by using it as a $1e^-$ substrate. Peroxidases may also promote NO consumption indirectly through generation of free radical species, which scavenge NO. Alternatively, NO may serve to modulate peroxidase catalytic activity. When serving as a substrate, NO may enhance catalytic rates by reducing compound II to form ferric enzyme, the rate-limiting step in the peroxidase cycle (*33*, *34*). NO may also promote alterations in substrate selectivity by influencing the distribution of peroxidase intermediates capable of executing $1e^-$ versus $2e^-$ oxidation reactions. Finally, NO may serve as a ligand for ferric peroxidases generating inactive Fe(III)−NO complexes.

ACKNOWLEDGMENT

We thank Dr. Dennis Stuehr for generous access to some of the instrumentation used for this study.

REFERENCES

1. Moncada, S., Palmer, R. M. J., and Higgs, F. A. (1991) *Pharmacol. Rev. 43*, 109−142.
2. Ignarro, L. J. (1990) *Annu. Rev. Pharmacol. Toxicol. 30*, 535−560.
3. Bredt, D. S., and Snyder, S. H. (1994) *Annu. Rev. Biochem. 63*, 175−195.
4. Barnes, P. J., Chung, K. F., and Page, C. P. (1998) *Pharmacol. Rev. 50*, 515−596.
5. Stuehr, D. J. (1999) *Biochim. Biophys. Acta 1411*, 217−230.

6. Persson M. G., Zetterstom, O., Agrenius, V, Ihre, E., and Gustafsson, L. E. (1994) *Lancet 343*, 146−147.
7. Kharitonov, S. A., Yates, D., Robbins, R. A., Logan-Sinclair, R., Shinebourne, E. A., and Barnes, P. J. (1994) *Lancet 343*, 133−135.
8. ten Hacken, N. H., van der Vaart, H., van der Mark, T. W., Koeter, G. H., and Postma, D. S. (1998) *Am. J. Respir. Crit. Care Med. 158*, 902−907.
9. Alving K., Weitzberg E., and Lundberg J. M. (1993) *Eur. Respir. J. 6*, 1368−1370.
10. National Heart, Lung, and Blood Institute. Expert Panel Report 2: Guidelines for the diagnosis and management of asthma (1997) National Institutes of Health Bethesda, MD, Publication No. 97-4051.
11. Saleh, D., Ernst, P., Lim, S., Barnes P. J., and Giaid, A. (1998) *FASEB J. 12*, 929−937.
12. Kaminsky, D. A., Mitchell, J., Carroll, N., James, A., Soultanakis, R., and Janssen, Y. (1999) *J. Allergy Clin. Immunol. 104*, 747−754.
13. Gaston, B., Sears, S., Woods, J., Hunt, J., Ponaman, M., McMahon, T., and Stamler, J. S. (1998) *Lancet 351*, 1317−1319.
14. Mitra, S. N., Slungaard, A., and Hazen, S. L. (2000) *Redox. Rep. 5*, 215−224.
15. Lancaster, J. R., Jr. (1994) *Proc. Natl. Acad. Sci. U.S.A. 91*, 8137−8141.
16. Wink, D. A., Hanbauer, I., Grisham, M. B., Laval, F., Nims, R. W., Laval, J., Cook, J., Pacelli, R., Liebmann, J., Krishna, M., Ford, P. C., and Mitchell, J. B. (1996) *Curr. Top. Cell Regul. 34*, 159−187.
17. Kharitonov, V. G., Sandquist, A. R., and Sharma V. S. (1994) *J. Biol. Chem. 269*, 5881−5883.
18. Beckman, J. S., and Koppenol, W. H. (1996) *Am. J. Physiol. 271*, C1424−C1437.
19. Ischiropoulos, H. (1998) *Arch. Biochem. Biophys. 356*, 1−11.
20. Sawa, T. Akaike, T., and Maeda H. (2000) *J. Biol. Chem. 275*, 3246−32474.
21. Reiter, C. D., Teng, R. J., and Beckman, J. S. (2000) *J. Biol. Chem. 275*, 32460−32466.
22. Darley-Usmar, V. M., Hogg, N., O'Leary, V. J., Wilson, M. T., and Moncada, S. (1992) *Free Radical Res. Commun. 17*, 9−20.
23. Radi, R., Beckman, J. S., Bush, K., M., and Freeman, B. A. (1991) *Arch. Biochem. Biophys. 288*, 481−487.
24. Hazen, S. L., Zhang, R., Shen, Z., Wu, W., Podrez, E. A., MacPherson, J. C., Schmitt, D., Mitra, S. N., Mukhopadhyay, C., Chen, Y., and Abu-Soud, H. M. (1999) *Circ. Res. 85*, 950−958.
25. Hogg, N., and Kalyanaraman, B. (1999) *Biochim. Biophys. Acta 1411*, 378−384.
26. MacPherson, J. C., Comhair, S. A. A., Erzurum, S. C., Klein, D. F., Lipscomb, M. F., Kavuru, M. S., Samoszuk, M., and Hazen, S. L. (2001) *J. Immunol. 166*, 5763−5772.
27. Chung, K. F., and Barnes, P. J. (1992) *Br. Med. Bull. 48*, 135−148.
28. Robinson, C., and Holgate, S. T. (1990) *Adv. Prostaglandin, Thromboxane, Leukotriene Res. 20*, 209−216.
29. O'Donnell, V. B., and Freeman, B. A. (2001) *Circ. Res. 88*, 12−21.
30. Abu-Soud, H. M., and Hazen, S. L. (2000) *J. Biol. Chem. 275*, 5425−5430.
31. Abu-Soud, H. M., and Hazen, S. L. (2000) *J. Biol. Chem. 275*, 37524−37532.
32. Dinauer, M. C., Nauseef, W. M., and Newburger, P. E. (2001) Inherited disorders of phagocyte killing, in *The metabolic and molecular bases of inherited diseases* (Scriver, C. R., et al., Eds.) pp 4857−4887, McGraw-Hill, New York.
33. Nauseef, W. M. (1998) *J. Mol. Med. 76*, 661−618.
34. Petrides, P. E., and Nauseef, W. M. (2000) *The peroxidase multi-gene family of enzymes: biochemical basis and clinical applications* (Petrides, P. E., and Nauseef, W. M., Eds.) Springer-Verlag, Berlin, Germany.
35. Kimura, S., and Ikeda-Saito, M. (1988) *Proteins: Struct., Funct., Genet. 3*, 113−120.
36. Ten, R. M., Pease, L. R., McKean, D. J., Bell, M. P., and Gleich, G. J. (1989) *J. Exp. Med. 169*, 1757−1769.
37. Kettle, A. J., and Winterbourn, C. C. (1997) *Redox. Rep. 3*, 3−15.
38. Klebanoff, S. J. (1999) *Proc. Assoc. Am. Physicians 111*, 383−389.
39. Weiss, S. J., Klein, R Slivka, A., and Wei, M. (1982) *J. Clin. Invest. 70*, 598−607.
40. Harrison, J. E., and Schultz, J. (1976) *J. Biol. Chem. 251*, 1371−1374.
41. Podrez, E. A., Abu-Soud, H. M., and Hazen S. L. (2000) *Free Radical Biol. Med. 28*, 1717−1725.
42. Weiss, S. J., Test, S. T, Eckmann, C. M., Roos, D., and Regiani, S. (1986) *Science 234*, 200−203.
43. Mayeno, A. N., Curran, A. J., Roberts, R. L., and Foote, C. S. (1989) *J. Biol. Chem. 264*, 5660−5668.
44. Wu, W., Chen, Y., d'Avignon, A., and Hazen, S. L. (1999) *Biochemistry 38*, 3538−3548.
45. Arlandson, M., Decker, T., Roongta, V. A., Bonilla, L., Mayo, K. H., MacPherson, J. C., Hazen, S. L., and Slungaard A. (2001) *J. Biol. Chem. 276*, 215−224.
46. Thomas, E. L., Milligan, T. W., Joyner, R. E., and Jefferson, M. M. (1994) *Infect. Immun. 62*, 529−535.
47. Wu, W., Samoszuk, M. K., Comhair, S. A., Thomassen, M. J., Farver, C. F., Dweik, R. A., Kavuru, M. S., Erzurum, S. C., and Hazen, S. L. (2000) *J. Clin. Invest. 105*, 1455−1463.
48. Holt, P. G., Macaubas, C., Stumbles, P. A., and Sly, P. D. (1999) *Nature 402*, B12−B17.
49. Gleich, G. J., Ottesen, E. A., Leiferman, K. M., and Ackerman, S. J. (1989) *Int. Arch. Allergy Appl. Immunol. 88*, 59−62.
50. Matthias, S., Holderby, M., Forteza, R., Abraham, W. M., Wanner, A., and Conner, G. E. (1977) *Am. J. Respir. Cell Mol. Biol. 17*, 97−105.
51. Rothenberg, M. E. (1998) *N. Engl. J. Med. 338*, 1592−1600.
52. Jorg, A., Pasquier, J.-M., and Klebanoff, S. J. (1982) *Biochim. Biophys. Acta 701*, 185−191.
53. Wu, W., Chen, Y., and Hazen, S. L. (1999) *J. Biol. Chem. 274*, 25933−25944.
54. Klebanoff, S. J., Waltersdorph, A. M., and Rosen, H. (1984) *Methods Enzymol. 105*, 399−403.
55. Rakita, R. M., Michel, B. R., and Rosen, H (1990) *Biochemistry 29*, 1075−1080.
56. van Dalen, C. J., Whitehouse, M. W., Winterbourn, C. C., and Kettle, A. J. (1997) *Biochem. J. 327*, 487−492.
57. Agner, K. (1963) *Acta Chem. Scand. 17*, S332−S338.
58. Bolscher, B. G. J. M., Plat, H., and Wever, R. (1984) *Biochim. Biophys. Acta 784*, 177−186.
59. Carlson, M. G., Peterson, C. G., and Venge, P. (1985) *J. Immunol. 134*, 1875−1879.
60. Babior, B. M., Kipnes, R. S., and Curnutte, J. T. (1973) *J. Clin. Invest. 52*, 741−744.
61. Agani, F. H., Kuo, N. T., Chang, C. H., Dreshaj, I. A., Farver, C. F., Krause, J. E., Ernsberger, P., Haxhiu, M. A., and Martin, R. J. (1997) *Am. J. Physiol. 273*, L40−L45.
62. Mhanna, M. J., Ferkol, T., Martin, R. J., Dreshaj, I. A., van Heeckeren, A. M., Kelley, T. J., and Haxhiu, M. A. (2001) *Med. J. Resp. Cell Mol. Biol.* (in press).
63. Furtmuller, P. G., Burner, U., Regelsberger, G., and Obinger, C. (2000) *Biochemistry 39*, 15578−15584.
64. Burner, U., Furtmuller, P. G., Kettle, A. J., Koppenol, W. H., and Obinger, C. (2000) *J. Biol. Chem. 275*, 20597−20601.
65. Marquez, L. A., and Dunford, H. B. (1995) *J. Biol. Chem. 270*, 30434−30440.
66. Kimura, S., and Yamazaki, I. (1979) *Arch. Biochem. Biophys. 198*, 580−588.
67. Marquez, L. A., Huang, J. T., and Dunford, H. B. (1994) *Biochemistry 33*, 1447−1454.
68. Abu-Soud, H. M., and Hazen, S. L. (2001) *Biochemistry* (in press).
69. Dweik, R. A., Comhair, S. A. A., Gaston, B., Thunnissen, F. B. J., Farver, C., Thomassen, M. J., Kavuru, M., Hammel, J., Abu-Soud, H. M., and Erzurum, S. C. (2001) *Proc. Natl. Acad. Sci. U.S.A. 98*, 2622−2627.

70. Gibson, P. G., Henry, R. L., and Thomas, P. (2000) *Eur. Respir. J. 16*, 1008−1015.
71. Antczak, A., Nowak, D., Bialasiewicz, P., and Kasielski, M. (1999) *Arch. Immunol. Ther. Exp. 47*, 119−126.
72. Dohlman, A. W., Black, H. R., and Royall, J. A. (1993) *Am. Rev. Respir. Dis. 148*, 955−960.
73. Stamler, J. S., Singel, D. J., and Loscalzo, J. (1992) *Science 258*, 1898−1902.
74. Glover, R. E., Koshkin, V., Dunford, H. B., and Mason, R. P. (1999) *Nitric Oxide 3*, 439−444.
75. van der Vliet, A., Eiserich, J. P., Halliwell, B., and Cross, C. E. (1997) *J. Biol. Chem. 272*, 7617−7625.
76. Eiserich, J. P., Hristova, M., Cross, C. E., Jones, A. D., Freeman, B. A., Halliwell, B., and van der Vliet, A. (1998) *Nature 391*, 393−397.
77. Schmitt, D., Shen, Z., Zhang, R., Colles, S. M., Wu, W., Salomon, R. G., Chen, Y., Chisolm, G. M., and Hazen, S. L. (1999) *Biochemistry 38*, 16904−16915.
78. Podrez, E. A., Schmitt, D., Hoff, H., and Hazen, S. L. (1999) *J. Clin. Invest. 103*, 1547−1560.
79. Sharma, V. S., Isaacson, R. A., John, M. E., Waterman, M. R., and Chevion, M. (1983) *Biochemistry 22*, 3897−3902.
80. Sharma, V. S., Traylor, T. G., and Gradiner, R. (1987) *Biochemistry 26*, 3837−3843.
81. Abu-Soud, H. M., Wang, J., Rousseau, D. L., Fukuto, J. M., Ignarro, L. J., and Stuehr, D. J. (1995) *J. Biol. Chem. 270*, 22997−23006.
82. Abu-Soud, H. M., Wu, C., Ghosh, K. D., and Stuehr, D. J. (1998) *Biochemistry 37*, 3777−3786.
83. Abu-Soud, H. M., Ichimori, K., Presta, A., and Stuehr, D. J. (2000) *J. Biol. Chem. 275*, 17349−17357.
84. Stone, J. R., and Marletta, M. A. (1996) *Biochemistry 35*, 1093−1099.
85. Hurst, J. K. (1991) Myleperoxidase-active site structure and catalytic mechanisms, in *Peroxidases in Chemistry and Biology* (Everse, J., Everse, K., and Grisham, M. B., Eds.) 1st ed., pp 37−62, CRC Press, Boca Raton, FL.

BI011206V